

Measurement of Associated Production of Z Bosons with Charm Quark Jets in $p\bar{p}$ Collisions at $\sqrt{s} = 1.96$ TeV

V. M. Abazov,³¹ B. Abbott,⁶⁶ B. S. Acharya,²⁵ M. Adams,⁴⁵ T. Adams,⁴³ J. P. Agnew,⁴⁰ G. D. Alexeev,³¹ G. Alkhazov,³⁵ A. Alton,^{55,*} A. Askew,⁴³ S. Atkins,⁵³ K. Augsten,⁷ C. Avila,⁵ F. Badaud,¹⁰ L. Bagby,⁴⁴ B. Baldin,⁴⁴ D. V. Bandurin,⁴³ S. Banerjee,²⁵ E. Barberis,⁵⁴ P. Baringer,⁵² J. F. Bartlett,⁴⁴ U. Bassler,¹⁵ V. Bazterra,⁴⁵ A. Bean,⁵² M. Begalli,² L. Bellantoni,⁴⁴ S. B. Beri,²³ G. Bernardi,¹⁴ R. Bernhard,¹⁹ I. Bertram,³⁸ M. Besançon,¹⁵ R. Beuselinck,³⁹ P. C. Bhat,⁴⁴ S. Bhatia,⁵⁷ V. Bhatnagar,²³ G. Blazey,⁴⁶ S. Blessing,⁴³ K. Bloom,⁵⁸ A. Boehnlein,⁴⁴ D. Boline,⁶³ E. E. Boos,³³ G. Borissov,³⁸ A. Brandt,⁶⁹ O. Brandt,²⁰ R. Brock,⁵⁶ A. Bross,⁴⁴ D. Brown,¹⁴ X. B. Bu,⁴⁴ M. Buehler,⁴⁴ V. Buescher,²¹ V. Bunichev,³³ S. Burdin,^{38,†} C. P. Buszello,³⁷ E. Camacho-Pérez,²⁸ B. C. K. Casey,⁴⁴ H. Castilla-Valdez,²⁸ S. Caughron,⁵⁶ S. Chakrabarti,⁶³ K. M. Chan,⁵⁰ A. Chandra,⁷¹ E. Chapon,¹⁵ G. Chen,⁵² S. W. Cho,²⁷ S. Choi,²⁷ B. Choudhary,²⁴ S. Cihangir,⁴⁴ D. Claes,⁵⁸ J. Clutter,⁵² M. Cooke,⁴⁴ W. E. Cooper,⁴⁴ M. Corcoran,⁷¹ F. Couderc,¹⁵ M.-C. Cousinou,¹² D. Cutts,⁶⁸ A. Das,⁴¹ G. Davies,³⁹ S. J. de Jong,^{29,30} E. De La Cruz-Burelo,²⁸ F. Déliot,¹⁵ R. Demina,⁶² D. Denisov,⁴⁴ S. P. Denisov,³⁴ S. Desai,⁴⁴ C. Deterre,^{20,‡} K. DeVaughan,⁵⁸ H. T. Diehl,⁴⁴ M. Diesburg,⁴⁴ P. F. Ding,⁴⁰ A. Dominguez,⁵⁸ A. Dubey,²⁴ L. V. Dudko,³³ A. Duperrin,¹² S. Dutt,²³ M. Eads,⁴⁶ D. Edmunds,⁵⁶ J. Ellison,⁴² V. D. Elvira,⁴⁴ Y. Enari,¹⁴ H. Evans,⁴⁸ V. N. Evdokimov,³⁴ L. Feng,⁴⁶ T. Ferbel,⁶² F. Fiedler,²¹ F. Filthaut,^{29,30} W. Fisher,⁵⁶ H. E. Fisk,⁴⁴ M. Fortner,⁴⁶ H. Fox,³⁸ S. Fuess,⁴⁴ A. Garcia-Bellido,⁶² J. A. García-González,²⁸ V. Gavrilov,³² W. Geng,^{12,56} C. E. Gerber,⁴⁵ Y. Gershtein,⁵⁹ G. Ginther,^{44,62} G. Golovanov,³¹ P. D. Grannis,⁶³ S. Greder,¹⁶ H. Greenlee,⁴⁴ G. Grenier,¹⁷ Ph. Gris,¹⁰ J.-F. Grivaz,¹³ A. Grohsjean,^{15,§} S. Grünendahl,⁴⁴ M. W. Grünewald,²⁶ T. Guillemain,¹³ G. Gutierrez,⁴⁴ P. Gutierrez,⁶⁶ J. Haley,⁵⁴ L. Han,⁴ K. Harder,⁴⁰ A. Harel,⁶² J. M. Hauptman,⁵¹ J. Hays,³⁹ T. Head,⁴⁰ T. Hebbeker,¹⁸ D. Hedin,⁴⁶ H. Hegab,⁶⁷ A. P. Heinson,⁴² U. Heintz,⁶⁸ C. Hensel,²⁰ I. Heredia-De La Cruz,^{28,‡} K. Herner,⁴⁴ G. Hesketh,^{40,||} M. D. Hildreth,⁵⁰ R. Hirosky,⁷² T. Hoang,⁴³ J. D. Hobbs,⁶³ B. Hoeneisen,⁹ J. Hogan,⁷¹ M. Hohlfeld,²¹ J. L. Holzbauer,⁵⁷ I. Howley,⁶⁹ Z. Hubacek,^{7,15} V. Hynek,⁷ I. Iashvili,⁶¹ Y. Ilchenko,⁷⁰ R. Illingworth,⁴⁴ A. S. Ito,⁴⁴ S. Jabeen,⁶⁸ M. Jaffré,¹³ A. Jayasinghe,⁶⁶ M. S. Jeong,²⁷ R. Jesik,³⁹ P. Jiang,⁴ K. Johns,⁴¹ E. Johnson,⁵⁶ M. Johnson,⁴⁴ A. Jonckheere,⁴⁴ P. Jonsson,³⁹ J. Joshi,⁴² A. W. Jung,⁴⁴ A. Juste,³⁶ E. Kajfasz,¹² D. Karmanov,³³ I. Katsanos,⁵⁸ R. Kehoe,⁷⁰ S. Kermiche,¹² N. Khalatyan,⁴⁴ A. Khanov,⁶⁷ A. Kharchilava,⁶¹ Y. N. Kharzhevich,³¹ I. Kiselevich,³² J. M. Kohli,²³ A. V. Kozelov,³⁴ J. Kraus,⁵⁷ A. Kumar,⁶¹ A. Kupco,⁸ T. Kurča,¹⁷ V. A. Kuzmin,³³ S. Lammers,⁴⁸ P. Lebrun,¹⁷ H. S. Lee,²⁷ S. W. Lee,⁵¹ W. M. Lee,⁴³ X. Lei,⁴¹ J. Lellouch,¹⁴ D. Li,¹⁴ H. Li,⁷² L. Li,⁴² Q. Z. Li,⁴⁴ J. K. Lim,²⁷ D. Lincoln,⁴⁴ J. Linnemann,⁵⁶ V. V. Lipaev,³⁴ R. Lipton,⁴⁴ H. Liu,⁷⁰ Y. Liu,⁴ A. Lobodenko,³⁵ M. Lokajicek,⁸ R. Lopes de Sa,⁶³ R. Luna-Garcia,^{28,¶} A. L. Lyon,⁴⁴ A. K. A. Maciel,¹ R. Madar,¹⁹ R. Magaña-Villalba,²⁸ S. Malik,⁵⁸ V. L. Malyshev,³¹ J. Mansour,²⁰ J. Martínez-Ortega,²⁸ R. McCarthy,⁶³ C. L. McGivern,⁴⁰ M. M. Meijer,^{29,30} A. Melnitchouk,⁴⁴ D. Menezes,⁴⁶ P. G. Mercadante,³ M. Merkin,³³ A. Meyer,¹⁸ J. Meyer,^{20,**} F. Miconi,¹⁶ N. K. Mondal,²⁵ M. Mulhearn,⁷² E. Nagy,¹² M. Narain,⁶⁸ R. Nayyar,⁴¹ H. A. Neal,⁵⁵ J. P. Negret,⁵ P. Neustroev,³⁵ H. T. Nguyen,⁷² T. Nunnemann,²² J. Orduna,⁷¹ N. Osman,¹² J. Osta,⁵⁰ A. Pal,⁶⁹ N. Parashar,⁴⁹ V. Parihar,⁶⁸ S. K. Park,²⁷ R. Partridge,^{68,††} N. Parua,⁴⁸ A. Patwa,^{64,‡‡} B. Penning,⁴⁴ M. Perfilov,³³ Y. Peters,²⁰ K. Petridis,⁴⁰ G. Petrillo,⁶² P. Pétrouff,¹³ M.-A. Pleier,⁶⁴ V. M. Podstavkov,⁴⁴ A. V. Popov,³⁴ M. Prewitt,⁷¹ D. Price,⁴⁸ N. Prokopenko,³⁴ J. Qian,⁵⁵ A. Quadt,²⁰ B. Quinn,⁵⁷ P. N. Ratoff,³⁸ I. Razumov,³⁴ I. Ripp-Baudot,¹⁶ F. Rizatdinova,⁶⁷ M. Rominsky,⁴⁴ A. Ross,³⁸ C. Royon,¹⁵ P. Rubinov,⁴⁴ R. Ruchti,⁵⁰ G. Sajot,¹¹ A. Sánchez-Hernández,²⁸ M. P. Sanders,²² A. S. Santos,^{1,§§} G. Savage,⁴⁴ L. Sawyer,⁵³ T. Scanlon,³⁹ R. D. Schamberger,⁶³ Y. Scheglov,³⁵ H. Schellman,⁴⁷ C. Schwanenberger,⁴⁰ R. Schwienhorst,⁵⁶ J. Sekaric,⁵² H. Severini,⁶⁶ E. Shabalina,²⁰ V. Shary,¹⁵ S. Shaw,⁵⁶ A. A. Shchukin,³⁴ V. Simak,⁷ P. Skubic,⁶⁶ P. Slattery,⁶² D. Smirnov,⁵⁰ G. R. Snow,⁵⁸ J. Snow,⁶⁵ S. Snyder,⁶⁴ S. Söldner-Rembold,⁴⁰ L. Sonnenschein,¹⁸ K. Soustruznik,⁶ J. Stark,¹¹ D. A. Stoyanova,³⁴ M. Strauss,⁶⁶ L. Suter,⁴⁰ P. Svoisky,⁶⁶ M. Titov,¹⁵ V. V. Tokmenin,³¹ Y.-T. Tsai,⁶² D. Tsybychev,⁶³ B. Tuchming,¹⁵ C. Tully,⁶⁰ L. Uvarov,³⁵ S. Uvarov,³⁵ S. Uzunyan,⁴⁶ R. Van Kooten,⁴⁸ W. M. van Leeuwen,²⁹ N. Varelas,⁴⁵ E. W. Varnes,⁴¹ I. A. Vasilyev,³⁴ A. Y. Verkhnev,³¹ L. S. Vertogradov,³¹ M. Verzocchi,⁴⁴ M. Vesterinen,⁴⁰ D. Vilanova,¹⁵ P. Vokac,⁷ H. D. Wahl,⁴³ M. H. L. S. Wang,⁴⁴ J. Warchol,⁵⁰ G. Watts,⁷³ M. Wayne,⁵⁰ J. Weichert,²¹ L. Welty-Rieger,⁴⁷ M. R. J. Williams,⁴⁸ G. W. Wilson,⁵² M. Wobisch,⁵³ D. R. Wood,⁵⁴ T. R. Wyatt,⁴⁰ Y. Xie,⁴⁴ R. Yamada,⁴⁴ S. Yang,⁴ T. Yasuda,⁴⁴ Y. A. Yatsunenko,³¹ W. Ye,⁶³ Z. Ye,⁴⁴ H. Yin,⁴⁴ K. Yip,⁶⁴ S. W. Youn,⁴⁴ J. M. Yu,⁵⁵ J. Zennaro,⁶¹ T. G. Zhao,⁴⁰ B. Zhou,⁵⁵ J. Zhu,⁵⁵ M. Zielinski,⁶² D. Zieminska,⁴⁸ and L. Zivkovic¹⁴

(The D0 Collaboration)

¹LAFEX, Centro Brasileiro de Pesquisas Físicas, Rio de Janeiro, Brazil

²Universidade do Estado do Rio de Janeiro, Rio de Janeiro, Brazil

- ³Universidade Federal do ABC, Santo André, Brazil
- ⁴University of Science and Technology of China, Hefei, People's Republic of China
- ⁵Universidad de los Andes, Bogotá, Colombia
- ⁶Charles University, Faculty of Mathematics and Physics, Center for Particle Physics, Prague, Czech Republic
- ⁷Czech Technical University in Prague, Prague, Czech Republic
- ⁸Institute of Physics, Academy of Sciences of the Czech Republic, Prague, Czech Republic
- ⁹Universidad San Francisco de Quito, Quito, Ecuador
- ¹⁰LPC, Université Blaise Pascal, CNRS/IN2P3, Clermont, France
- ¹¹LPSC, Université Joseph Fourier Grenoble 1, CNRS/IN2P3, Institut National Polytechnique de Grenoble, Grenoble, France
- ¹²CPPM, Aix-Marseille Université, CNRS/IN2P3, Marseille, France
- ¹³LAL, Université Paris-Sud, CNRS/IN2P3, Orsay, France
- ¹⁴LPNHE, Universités Paris VI and VII, CNRS/IN2P3, Paris, France
- ¹⁵CEA, Irfu, SPP, Saclay, France
- ¹⁶IPHC, Université de Strasbourg, CNRS/IN2P3, Strasbourg, France
- ¹⁷IPNL, Université Lyon 1, CNRS/IN2P3, Villeurbanne, France and Université de Lyon, Lyon, France
- ¹⁸III. Physikalisches Institut A, RWTH Aachen University, Aachen, Germany
- ¹⁹Physikalisches Institut, Universität Freiburg, Freiburg, Germany
- ²⁰II. Physikalisches Institut, Georg-August-Universität Göttingen, Göttingen, Germany
- ²¹Institut für Physik, Universität Mainz, Mainz, Germany
- ²²Ludwig-Maximilians-Universität München, München, Germany
- ²³Panjab University, Chandigarh, India
- ²⁴Delhi University, Delhi, India
- ²⁵Tata Institute of Fundamental Research, Mumbai, India
- ²⁶University College Dublin, Dublin, Ireland
- ²⁷Korea Detector Laboratory, Korea University, Seoul, Korea
- ²⁸CINVESTAV, Mexico City, Mexico
- ²⁹Nikhef, Science Park, Amsterdam, the Netherlands
- ³⁰Radboud University Nijmegen, Nijmegen, the Netherlands
- ³¹Joint Institute for Nuclear Research, Dubna, Russia
- ³²Institute for Theoretical and Experimental Physics, Moscow, Russia
- ³³Moscow State University, Moscow, Russia
- ³⁴Institute for High Energy Physics, Protvino, Russia
- ³⁵Petersburg Nuclear Physics Institute, St. Petersburg, Russia
- ³⁶Institució Catalana de Recerca i Estudis Avançats (ICREA) and Institut de Física d'Altes Energies (IFAE), Barcelona, Spain
- ³⁷Uppsala University, Uppsala, Sweden
- ³⁸Lancaster University, Lancaster LA1 4YB, United Kingdom
- ³⁹Imperial College London, London SW7 2AZ, United Kingdom
- ⁴⁰The University of Manchester, Manchester M13 9PL, United Kingdom
- ⁴¹University of Arizona, Tucson, Arizona 85721, USA
- ⁴²University of California Riverside, Riverside, California 92521, USA
- ⁴³Florida State University, Tallahassee, Florida 32306, USA
- ⁴⁴Fermi National Accelerator Laboratory, Batavia, Illinois 60510, USA
- ⁴⁵University of Illinois at Chicago, Chicago, Illinois 60607, USA
- ⁴⁶Northern Illinois University, DeKalb, Illinois 60115, USA
- ⁴⁷Northwestern University, Evanston, Illinois 60208, USA
- ⁴⁸Indiana University, Bloomington, Indiana 47405, USA
- ⁴⁹Purdue University Calumet, Hammond, Indiana 46323, USA
- ⁵⁰University of Notre Dame, Notre Dame, Indiana 46556, USA
- ⁵¹Iowa State University, Ames, Iowa 50011, USA
- ⁵²University of Kansas, Lawrence, Kansas 66045, USA
- ⁵³Louisiana Tech University, Ruston, Louisiana 71272, USA
- ⁵⁴Northeastern University, Boston, Massachusetts 02115, USA
- ⁵⁵University of Michigan, Ann Arbor, Michigan 48109, USA
- ⁵⁶Michigan State University, East Lansing, Michigan 48824, USA
- ⁵⁷University of Mississippi, University, Mississippi 38677, USA
- ⁵⁸University of Nebraska, Lincoln, Nebraska 68588, USA
- ⁵⁹Rutgers University, Piscataway, New Jersey 08855, USA
- ⁶⁰Princeton University, Princeton, New Jersey 08544, USA
- ⁶¹State University of New York, Buffalo, New York 14260, USA
- ⁶²University of Rochester, Rochester, New York 14627, USA

⁶³State University of New York, Stony Brook, New York 11794, USA⁶⁴Brookhaven National Laboratory, Upton, New York 11973, USA⁶⁵Langston University, Langston, Oklahoma 73050, USA⁶⁶University of Oklahoma, Norman, Oklahoma 73019, USA⁶⁷Oklahoma State University, Stillwater, Oklahoma 74078, USA⁶⁸Brown University, Providence, Rhode Island 02912, USA⁶⁹University of Texas, Arlington, Texas 76019, USA⁷⁰Southern Methodist University, Dallas, Texas 75275, USA⁷¹Rice University, Houston, Texas 77005, USA⁷²University of Virginia, Charlottesville, Virginia 22904, USA⁷³University of Washington, Seattle, Washington 98195, USA

(Received 20 August 2013; published 27 January 2014)

We present the first measurements of the ratios of cross sections $\sigma(p\bar{p} \rightarrow Z + c \text{ jet})/\sigma(p\bar{p} \rightarrow Z + \text{jet})$ and $\sigma(p\bar{p} \rightarrow Z + c \text{ jet})/\sigma(p\bar{p} \rightarrow Z + b \text{ jet})$ for the associated production of a Z boson with at least one charm or bottom quark jet. Jets have transverse momentum $p_T^{\text{jet}} > 20$ GeV and pseudorapidity $|\eta^{\text{jet}}| < 2.5$. These cross section ratios are measured differentially as a function of jet and Z boson transverse momenta, based on 9.7 fb^{-1} of $p\bar{p}$ collisions collected with the D0 detector at the Fermilab Tevatron Collider at $\sqrt{s} = 1.96$ TeV. The measurements show significant deviations from perturbative QCD calculations and predictions from various event generators.

DOI: 10.1103/PhysRevLett.112.042001

PACS numbers: 12.38.Qk, 13.85.Qk, 14.65.Dw, 14.70.Hp

Studies of Z boson production in association with heavy flavor (HF) jets originating from b or c quarks provide important tests of perturbative quantum chromodynamics (pQCD) calculations [1]. A good theoretical description of these processes is essential since they form a major background for a variety of physics processes, including standard model Higgs boson production in association with a Z boson, $ZH(H \rightarrow b\bar{b})$ [2]. Furthermore, the relative contributions of the different flavors to the background is important since $Z + c$ jet events can be misidentified as $Z + b$ jet events, or vice versa, and, therefore, introduce additional uncertainties into measurements.

The ratio of $Z + b$ jet to inclusive $Z + \text{jet}$ production cross sections for events with one or more jets has previously been measured by the CDF [3,4] and D0 [5,6] Collaborations. This Letter reports the first measurement of associated charm jet production with a Z boson. We present the measurement of the ratio of cross sections for $Z + c$ jet to $Z + \text{jet}$ production as well as $Z + c$ jet to $Z + b$ jet production in events with at least one jet. The current analysis is based on the complete Run II data sample collected using the D0 detector [7] at Fermilab's Tevatron $p\bar{p}$ Collider with a center-of-mass energy of 1.96 TeV, and corresponds to an integrated luminosity of 9.7 fb^{-1} following the application of relevant data quality requirements. The measurement of the ratio of cross sections benefits from the cancellation of several systematic uncertainties and, therefore, allows for a more precise comparison of data with theoretical predictions. These ratio measurements are also presented differentially as a function of the transverse momenta of the jet (p_T^{jet}) and Z boson (p_T^Z).

We use the same triggering, selections, object reconstruction, and event modeling as described in the recent D0 measurement of $Z + b$ jet production [6], but with a dedicated strategy for the extraction of the c -jet fraction. Events must contain a $Z \rightarrow \ell\ell$ candidate with a dilepton invariant mass in the range $70 < M_{\ell\ell} < 110$ GeV ($\ell = e, \mu$).

Dielectron (ee) events are required to have two electrons, with no requirement on the sign of their electric charge, with transverse momentum $p_T > 15$ GeV identified through electromagnetic showers in the calorimeter. One electron must be identified within a pseudorapidity [8] region $|\eta| < 1.1$, while the second electron can be reconstructed in the region $|\eta| < 2.5$. Dimuon ($\mu\mu$) events are required to have two oppositely charged muons, with $p_T > 15$ GeV and $|\eta| < 2$. In addition, at least one hadronic jet must be reconstructed in the event using an iterative midpoint cone algorithm [9] with a cone size of $\Delta R = \sqrt{(\Delta\phi)^2 + (\Delta y)^2} = 0.5$ where ϕ is the azimuthal angle and y is the rapidity. This jet must satisfy $p_T^{\text{jet}} > 20$ GeV and $|\eta^{\text{jet}}| < 2.5$.

Several processes can mimic the signature of $Z + \text{jet}$ events. These include top quark pair ($t\bar{t}$), diboson (WW , WZ , and ZZ), and multijet production. To suppress the contributions from $t\bar{t}$ production, events with significant imbalance in the measured transverse energy E_T , due to undetected neutrinos from the W boson decay ($t \rightarrow Wb \rightarrow \ell\nu_\ell b$), are rejected if $E_T > 60$ GeV. These selection criteria retain an inclusive sample of 176 498 $Z + \text{jet}$ event candidates in the ee and $\mu\mu$ channels.

To estimate acceptances, efficiencies, and backgrounds, the $Z + \text{jet}$ events (including HF jets) and $t\bar{t}$ events are modeled by ALPGEN [10], which generates subprocesses using higher-order QCD tree-level matrix elements,

interfaced with the PYTHIA Monte Carlo (MC) event generator [11] for parton showering and hadronization and EVTGEN [12] for modeling the decay of particles containing b and c quarks. Inclusive diboson production is simulated with PYTHIA. The CTEQ6L1 [13] parton distribution functions (PDFs) are used in these simulations and the cross sections are scaled to the corresponding higher-order theoretical calculations [6]. The multijet background, where jets are misidentified as leptons, is determined using a data-driven method [6]. The fractions of non- $Z + \text{jet}$ events in the ee and $\mu\mu$ samples are 9.6% and 1.3%, respectively. These fractions are dominated by multijet production where a jet is either misreconstructed as a lepton in the electron channel, or a lepton from decays of hadrons in a jet that passes the isolation requirement, in the muon channel.

This analysis uses a two-step procedure to determine the HF content of jets in the selected $Z + \text{jet}$ events. We employ a HF tagging algorithm [14] to enrich the sample in b and c jets. The b , c , and light jet composition of the data is then extracted via a template-based fit.

Jets considered for HF tagging are subject to a preselection requirement, known as “taggability” [14], to decouple the intrinsic performance of the HF jet tagging algorithm from effects related to track reconstruction efficiency. The jet is required to have at least two associated tracks with $p_T > 0.5$ GeV and the highest- p_T track must have $p_T > 1$ GeV. The efficiency of the taggability requirement is 90% for both c and b jets.

The HF tagging algorithm is based on a multivariate analysis (MVA) technique [15] that provides an improved performance over the neural network HF tagging discriminant, described in Ref. [14], used in earlier D0 analyses. This new algorithm (MVA_{bl}) also utilizes the relatively long lifetime of HF hadrons with respect to their lighter counterparts. Events with at least one jet passing the HF tagging selection are considered in the analysis.

To extract the fraction of different flavor jets in the data sample, a second discriminant, D_{MJL} , is employed, which offers improved flavor separation for jets passing our MVA_{bl} requirement [6]. It combines two discriminating variables, the secondary vertex mass (M_{SV}) and the jet lifetime impact parameter (JLIP) [14]: $D_{\text{MJL}} = 0.5 \times (M_{\text{SV}}/5 \text{ GeV} - \ln(\text{JLIP})/20)$. The coefficients in this expression are chosen to optimize the separation of the HF and light quark components. Figure 1(a) shows the D_{MJL} distributions (templates) obtained from simulations of all three considered jet flavors that pass an MVA_{bl} requirement.

To measure the relative fraction of c jets in the HF enriched sample, two approaches were considered. The first is based on the methods used in Ref. [6] where the composition of b , c , and light jets is extracted by fitting MC templates to the data. This approach yields a large uncertainty on the c -jet fraction since the D_{MJL} distributions of c and light jets are similar. The second approach is

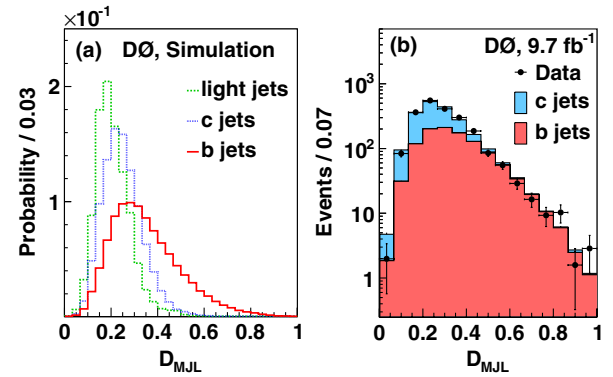


FIG. 1 (color online). (a) The probability densities of the D_{MJL} discriminant, normalized to unity, for b , c , and light jets passing the final selection requirements. These templates are obtained from MC simulations. (b) The D_{MJL} discriminant distribution of events in the combined sample after background subtraction. The distributions of the b and c jets are weighted by the fractions found from the fit. Uncertainties are statistical only.

to suppress events with light jets by employing a more stringent MVA_{bl} requirement. The remaining small $Z + \text{lightjet}$ contribution, as estimated with data-corrected simulations, is then subtracted from the D_{MJL} data distribution along with the other backgrounds. The corresponding D_{MJL} templates for QCD, top pair production, diboson, and $Z + \text{lightjets}$ are scaled to their estimated fractions in the final sample. This allows for the data to be fit with only b and c jet templates. Both methods yield consistent results, but the second method benefits from a reduced overall uncertainty as only the normalization of b and c jet templates are allowed to vary when fitting the data. Events are retained for further analysis if they contain at least one jet with an MVA_{bl} requirement. After these requirements, 2665 $Z + \text{jet}$ events are selected where only the highest- p_T HF tagged jet is examined. The efficiencies of the MVA_{bl} selection for b and c jets, and the light jet misidentification rate are 40%, 9.0%, and 0.24%, respectively. The background is dominated by $Z + \text{light jet}$ events that comprise 12% of the total sample. Before the two parameter fit, all background components are subtracted from the data, yielding a sample of 2125 events.

The remaining sample is mostly composed of $Z + b$ and $Z + c$ jet event candidates. The corresponding b and c jet fractions of events are measured in the ee and $\mu\mu$ samples separately, yielding c jet flavor fractions of $0.509 \pm 0.041(\text{stat})$ and $0.470 \pm 0.039(\text{stat})$, respectively. As these are consistent and the kinematics of the corresponding events are similar, we combine the two samples to increase the statistical power of the fit. The combined D_{MJL} distribution of the HF-enriched background subtracted data and the fitted templates for the b and c jets are shown in Fig. 1(b). The corresponding fractions of c and b jets in the data are found to be $0.486 \pm 0.027(\text{stat})$ and $0.514 \pm 0.027(\text{stat})$, respectively. These fractions are

combined with the relevant detector acceptances and efficiencies to determine the ratios of cross sections using

$$R_{c/\text{jet}} \equiv \frac{\sigma(Z + c \text{ jet})}{\sigma(Z + \text{jet})} = \frac{N_{\text{HF}} f_c}{N_{\text{incl}} \epsilon_{\text{tag}}^c} \times \frac{\mathcal{A}_{\text{incl}}}{\mathcal{A}_c},$$

$$R_{c/b} \equiv \frac{\sigma(Z + c \text{ jet})}{\sigma(Z + b \text{ jet})} = \frac{f_c \epsilon_{\text{tag}}^b}{f_b \epsilon_{\text{tag}}^c} \times \frac{\mathcal{A}_b}{\mathcal{A}_c}, \quad (1)$$

where N_{incl} is the total number of $Z + \text{jet}$ events before the tagging requirements, N_{HF} is the number of $Z + \text{jet}$ events used in the D_{MJL} fit, $f_{b(c)}$ is the extracted $b(c)$ jet fraction, and $\epsilon_{\text{tag}}^{b(c)}$ is the selection efficiency for $b(c)$ jets, which combines the efficiencies for taggability and MVA_{bl} discriminant selection. N_{incl} and N_{HF} correspond to the number of events that remain after the contributions from various background processes have been subtracted. We subtract contributions from $t\bar{t}$, diboson, and multijet production to obtain N_{incl} , while we also subtract the $Z + \text{light jet}$ events when calculating N_{HF} .

The differences in the detector acceptances for the inclusive jet $\mathcal{A}_{\text{incl}}$ and $b(c)$ jets $\mathcal{A}_{b(c)}$ are estimated from MC simulations in the kinematic region that satisfies the p_T and η [8] requirements for leptons and jets. For the differential measurements, the acceptances are obtained in bins of p_T^{jet} and p_T^Z , and account for the small residual migration effects that do not cancel in the ratio.

Using Eqs. (1), the ratio of the cross sections $Z + c \text{ jet}$ to inclusive $Z + \text{jet}$ in the combined $\mu\mu$ and ee channel, $R_{c/\text{jet}}$, is $0.0829 \pm 0.0052(\text{stat})$ and the ratio of cross sections $Z + c \text{ jet}$ to $Z + b \text{ jet}$, $R_{c/b}$, is found to be $4.00 \pm 0.21(\text{stat})$. These ratios have also been measured differentially as a function of p_T^{jet} and p_T^Z . For $R_{c/\text{jet}}$, the highest- p_T tagged jet from the HF enriched sample is used in the numerator, while the denominator uses the highest- p_T jet from the $Z + \text{jet}$ sample. The selected bin sizes along with the corresponding statistics of data events are listed in

TABLE I. Summary of bins, data statistics after final selection, and the measured ratios along with the statistical and systematic relative uncertainties in percent. Bin centers, shown in parenthesis, are chosen using the prescription in Ref. [16].

p_T^{jet} [GeV]	N_{HF}	$R_{c/\text{jet}}$	Stat		Syst		$R_{c/b}$	Stat		Syst	
			[%]	[%]	[%]	[%]		[%]	[%]	[%]	[%]
20–30 (24.6)	741	0.068	12	16	3.64	8.5	21				
30–40 (34.3)	525	0.084	11	12	3.97	8.3	14				
40–60 (47.3)	474	0.099	11	9.1	3.98	10	13				
60–200 (78.0)	380	0.085	13	11	4.30	13	14				
p_T^Z [GeV]											
0–20 (10.2)	285	0.041	29	22	1.15	26	32				
20–40 (29.5)	763	0.073	8.2	12	6.10	8.2	20				
40–60 (49.0)	588	0.104	10	11	5.06	10	15				
60–200 (92.7)	487	0.108	13	8.3	3.41	13	13				

Table I. In each case, all the quantities that enter into Eqs. (1) are determined in each bin.

Several systematic uncertainties cancel when the ratios are measured. These include those due to the luminosity measurement, trigger, lepton, and the jet reconstruction efficiencies. The remaining uncertainties are estimated separately for the integrated and differential results. For the two ratios the systematic uncertainties are estimated separately.

For the integrated $R_{c/\text{jet}}$ measurement, the largest systematic uncertainty of 8.1% comes from the estimation of the $Z + \text{light jet}$ background. This is quantified by comparing the fraction of $Z + \text{light jet}$ events extracted from data and simulations using a three-template (light, c , and b jet) fit. The amount of subtracted $Z + \text{light jet}$ events is varied by the corresponding uncertainty of 20%, and the difference in the final result is taken as a systematic uncertainty. This procedure has been repeated for various MVA_{bl} selections and demonstrates stability of the final result. The next largest systematic uncertainty comes from the shape of the D_{MJL} templates used in the fit. A variety of different aspects can affect the shape of the templates: two HF jets being reconstructed as a single jet, models of b and c quark fragmentation, the normalization of the subtracted background from the non- $Z + \text{jet}$ events, the difference in the shape of the light jet MC template and a template derived from a light jet enriched dijet data sample, and the uncertainty of shape of the templates due to MC statistics. These are all evaluated by varying the central values by the corresponding uncertainties, one at a time, and repeating the entire analysis chain, resulting in a 5.5% uncertainty. An additional uncertainty of 3.4% comes from jet energy calibration; it comprises the uncertainties on the jet energy resolution and the jet energy scale. An uncertainty is also associated with the c jet tagging efficiency (1.9%) [14]. Finally, a small contribution ($<0.1\%$) is coming from the dependence of the acceptance on modeling of the signal events. When summed in quadrature the total systematic uncertainty for the integrated $R_{c/\text{jet}}$ ratio is 10.6%. The corresponding total systematic uncertainty is 14.4% for $R_{c/b}$, and is larger compared to the uncertainty on $R_{c/\text{jet}}$ due to the strong correlation in the extracted b and c jet fractions from the two-template fit. Table I lists the total statistical and systematic uncertainties (added in quadrature) for the differential results. To account for bin correlations in the differential measurement each systematic effect is evaluated by varying the corresponding central values by their uncertainties before the entire analysis chain is repeated. Finally, for the integrated ratios we obtain values of $R_{c/\text{jet}} = 0.0829 \pm 0.0052(\text{stat}) \pm 0.0089(\text{syst})$ and $R_{c/b} = 4.00 \pm 0.21(\text{stat}) \pm 0.58(\text{syst})$.

The measurements are compared to predictions from an MCFM NLO pQCD calculation and three MC event generators, SHERPA [17], PYTHIA, and ALPGEN. The NLO predictions are based on MCFM [1], version 6.3, with the

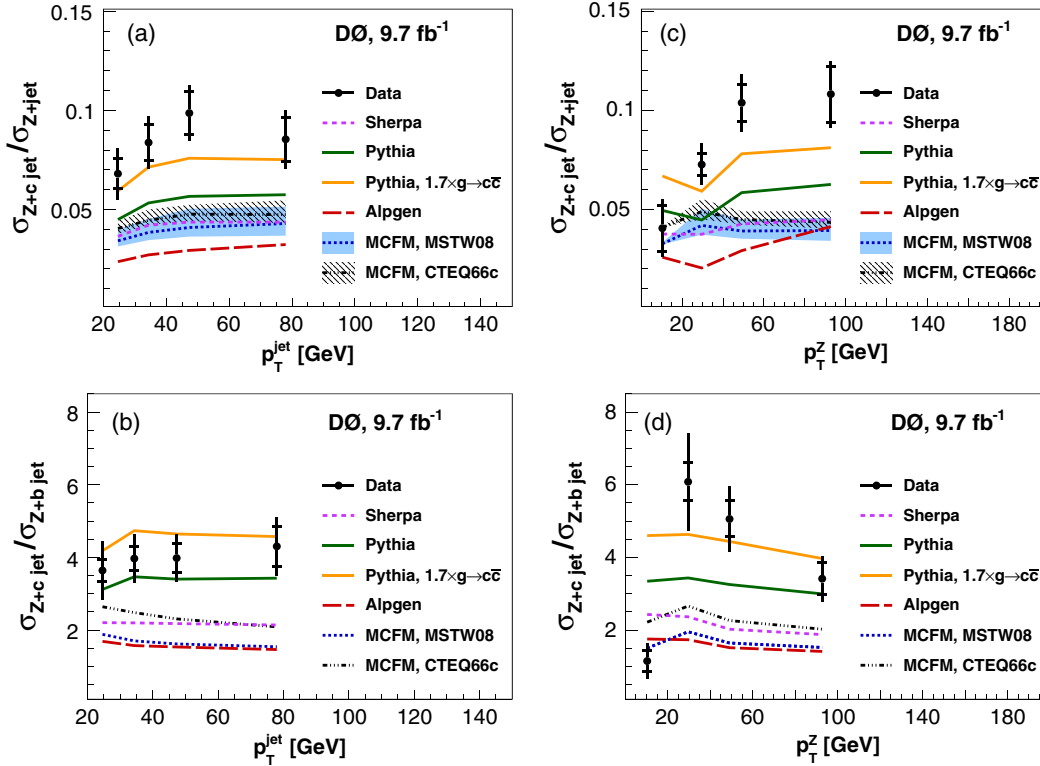


FIG. 2 (color online). Ratios of the cross sections $R_{c/\text{jet}}$ and $R_{c/b}$ as a function of (a),(b) p_T^{jet} and (c),(d) p_T^Z , respectively. The uncertainties on the data include statistical (inner error bar) and full uncertainties (entire error bar). Various predictions from theoretical models are also shown. The bands for MCFM predictions in $R_{c/\text{jet}}$ ratios represent variations of the scales up and down by a factor of 2. The corresponding uncertainties in $R_{c/b}$ (less than 4%) are not visible on this scale.

MSTW2008 PDFs [18] and the renormalization and factorization scales set at $\mu_R^2 = \mu_F^2 = M_Z^2 + p_{T,\text{total}}^2$. Here, M_Z is the Z boson mass and $p_{T,\text{total}}$ is the scalar sum of the transverse momentum for all the jets with $p_T^{\text{jet}} > 20$ GeV and $|\eta| < 2.5$ in the event. Corrections are applied to account for nonperturbative effects, on the order of 5%, estimated using the ALPGEN+PYTHIA simulation. The NLO pQCD predictions of $R_{c/\text{jet}} = 0.0368$ and $R_{c/b} = 1.64$ [1] disagree significantly with the measurements. In the case where the intrinsic charm of the proton is enhanced, as suggested in the CTEQ6.6c PDF sets [13], MCFM yields ratios of $R_{c/\text{jet}} = 0.0425$ and $R_{c/b} = 2.23$, which still disagree with our data.

The uncertainty on the $R_{c/\text{jet}}$ theoretical predictions is evaluated by simultaneously changing the μ_R and μ_F scales up and down by a factor of 2, yielding an uncertainty of up to 11% on $R_{c/\text{jet}}$, while this uncertainty cancels in $R_{c/b}$. However, this uncertainty is smaller than the effect due to the intrinsic charm enhancement, which is 15% and 36% for $R_{c/\text{jet}}$ and $R_{c/b}$, respectively.

The ratios of differential cross sections as a function of p_T^{jet} and p_T^Z are compared to various predictions in Fig. 2. On average, the NLO predictions significantly underestimate the data, by a factor of 2.5 for the integrated results. As for the MC event generators, PYTHIA predictions

are closer to data. An improved description can be achieved by enhancing the default rate of $g \rightarrow c\bar{c}$ in PYTHIA by a factor of 1.7, motivated by the $\gamma + c$ jet production measurements at the Tevatron [19,20].

The largest discrepancy between data and predictions, in particular for the shape of the differential distributions, is for $R_{c/b}$ as a function of p_T^Z [Fig. 2(d)]. The level of disagreement in shape is quantified for the MCFM NLO prediction when its integrated result is scaled up to match the data. We generated a large number of pseudoexperiments and found the p value for the four bins in p_T^Z to simultaneously fluctuate to the observed $R_{c/b}$ values (or beyond) to be 2%.

We have presented the first measurements of the ratios of integrated cross sections $\sigma(p\bar{p} \rightarrow Z + c \text{ jet})/\sigma(p\bar{p} \rightarrow Z + \text{jet})$ and $\sigma(p\bar{p} \rightarrow Z + c \text{ jet})/\sigma(p\bar{p} \rightarrow Z + b \text{ jet})$, as well as the ratios of the differential cross sections in bins of p_T^{jet} and p_T^Z , for events with a Z boson decaying to electrons or muons and at least one jet in the final state. Measurements are based on the data sample collected by the D0 experiment in run II of the Tevatron, corresponding to an integrated luminosity of 9.7 fb^{-1} at a center-of-mass energy of 1.96 TeV. For jets with $p_T^{\text{jet}} > 20$ GeV and $|\eta^{\text{jet}}| < 2.5$, the measured integrated ratios are $R_{c/\text{jet}} = 0.0829 \pm 0.0052(\text{stat}) \pm 0.0089(\text{syst})$, and

$R_{c/b} = 4.00 \pm 0.21(\text{stat}) \pm 0.58(\text{syst})$. The NLO pQCD predictions disagree significantly with the results. PYTHIA agrees better with the measured ratios, especially when the gluon splitting to $c\bar{c}$ pairs is enhanced.

We thank the authors of Refs. [1,17] for valuable discussions, and the staffs at Fermilab and collaborating institutions, and acknowledge support from the U.S. DOE and NSF (U.S.); CEA and CNRS/IN2P3 (France); MON, NRC KI, and RFBR (Russia); CNPq, FAPERJ, FAPESP, and FUNDUNESP (Brazil); DAE and DST (India); Colciencias (Colombia); CONACyT (Mexico); NRF (Korea); FOM (The Netherlands); STFC and the Royal Society (United Kingdom); MSMT and GACR (Czech Republic); BMBF and DFG (Germany); SFI (Ireland); The Swedish Research Council (Sweden); and CAS and CNSF (China).

*Visitor from Augustana College, Sioux Falls, South Dakota, USA.

†Visitor from The University of Liverpool, Liverpool, United Kingdom.

§Visitor from DESY, Hamburg, Germany.

‡Visitor from Universidad Michoacana de San Nicolas de Hidalgo, Morelia, Mexico.

††Visitor from SLAC, Menlo Park, California, USA.

‡‡Visitor from University College London, London, United Kingdom.

¶Visitor from Centro de Investigacion en Computacion-IPN, Mexico City, Mexico.

§§Visitor from Universidade Estadual Paulista, São Paulo, Brazil.

**Visitor from Karlsruher Institut für Technologie (KIT)-Steinbuch Centre for Computing (SCC).

‡‡‡Visitor from Office of Science, U.S. Department of Energy, Washington, D.C. 20585, USA.

- [1] J. M. Campbell, R. K. Ellis, F. Maltoni, and S. Willenbrock, *Phys. Rev. D* **69**, 074021 (2004).
 [2] V. M. Abazov *et al.* (D0 Collaboration), *Phys. Rev. Lett.* **109**, 121803 (2012); T. Aaltonen *et al.* (CDF Collaboration), *Phys. Rev. Lett.* **109**, 111803 (2012).

- [3] A. Abulencia *et al.* (CDF Collaboration), *Phys. Rev. D* **74**, 032008 (2006).
 [4] T. Aaltonen *et al.* (CDF Collaboration), *Phys. Rev. D* **79**, 052008 (2009).
 [5] V. M. Abazov *et al.* (D0 Collaboration), *Phys. Rev. Lett.* **94**, 161801 (2005).
 [6] V. M. Abazov *et al.* (D0 Collaboration), *Phys. Rev. D* **87**, 092010 (2013).
 [7] V. M. Abazov *et al.* (D0 Collaboration), *Nucl. Instrum. Methods Phys. Res., Sect. A* **565**, 463 (2006); M. Abolins *et al.*, *Nucl. Instrum. Methods Phys. Res., Sect. A* **584**, 75 (2008); R. Angstadt *et al.*, *Nucl. Instrum. Methods Phys. Res., Sect. A* **622**, 298 (2010).
 [8] Pseudorapidity is defined as $\eta = -\ln[\tan(\theta/2)]$, with the polar angle θ measured relative to the proton beam direction.
 [9] G. C. Blazey *et al.*, arXiv:hep-ex/0005012.
 [10] M. L. Mangano, F. Piccinini, A. D. Polosa, M. Moretti, and R. Pittau, *J. High Energy Phys.* **07** (2003) 001. Version 2.11 was used.
 [11] T. Sjöstrand, S. Mrenna, and P. Skands, *J. High Energy Phys.* **05** (2006) 026. Version 6.409 was used.
 [12] D. J. Lange, *Nucl. Instrum. Methods Phys. Res., Sect. A* **462**, 152 (2001).
 [13] J. Pumplin, D. R. Stump, J. Huston, H.-L. Lai, P. Nadolsky, and W.-K. Tung, *J. High Energy Phys.* **07** (2002) 012.
 [14] V. M. Abazov *et al.* (D0 Collaboration), *Nucl. Instrum. Methods Phys. Res., Sect. A* **620**, 490 (2010); V. M. Abazov *et al.* (D0 Collaboration), arXiv:1312.7623.
 [15] A. Hoecker, P. Speckmayer, J. Stelzer, J. Therhaag, E. von Toerne, and H. Voss, *Proc. Sci., ACAT* (2007) 040.
 [16] G. D. Lafferty, and T. R. Wyatt, *Nucl. Instrum. Methods Phys. Res., Sect. A* **355**, 541 (1995).
 [17] T. Gleisberg, S. Höche, F. Krauss, M. Schönherr, S. Schumann, F. Siegert, and J. Winter, *J. High Energy Phys.* **02** (2009) 007.
 [18] A. D. Martin, W. J. Stirling, R. S. Thorne, and G. Watt, *Eur. Phys. J. C* **63**, 189 (2009).
 [19] V. M. Abazov *et al.* (D0 Collaboration), *Phys. Lett. B* **719**, 354 (2013).
 [20] T. Aaltonen *et al.* (CDF Collaboration), *Phys. Rev. Lett.* **111**, 042003 (2013).